Experimental characterisation of a superconducting quantum interference device

THOMAS SCHANZER [a]

[a] *School of Physics, University of New South Wales, Sydney, Australia*

ABSTRACT: We present measurements of the key properties of a superconducting quantum interference device (SQUID), including the critical current threshold for superconductivity, the periodic oscillations in the voltage across the device with changing magnetic field and discrete Shapiro steps in voltage when a microwave-frequency electric field is applied. We establish rigorous techniques for analysing the relevant data that may be applied to other SQUIDs and sensitive magnetic field measurements.

1. Introduction

1a. Structure and key properties of the SQUID

A superconducting quantum interference device, or SQUID, consists of a superconducting ring, interrupted by two thin non-superconducting regions—Josephson junctions—on opposite sides, as shown in Figure 1. While a full quantum mechanical description of the device is beyond the scope of this report, we will briefly outline some of its key properties.

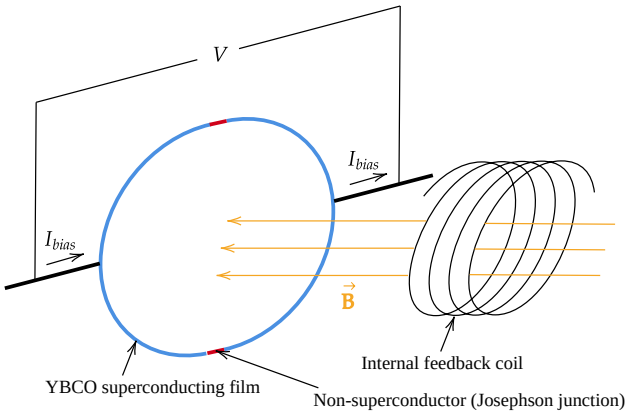

FIG. 1. Diagram of the SQUID used in this work.

A biasing current may be passed between the two sides of the coil. Below the critical temperature of the superconductor, the Josephson junctions create a current threshold, above which the ring will cease to superconduct and a potential difference V will develop between the two sides. If each junction has a critical current I_c, the critical current of the SQUID as a whole will be $2I_c$.

Secondly, due to the ring's superconductivity, the application of an external magnetic field induces a screening current that circulates in the ring to maintain zero magnetic flux through it; if the flux were to vary, a potential difference would appear in the loop in accordance with Faraday's law. This screening current is superimposed upon any biasing current passing through the ring, reducing the critical current. If the external magnetic field is increased further, the critical current may be exceeded, destroying the superconductivity, causing a voltage to develop across the loop and allowing some flux to enter. It may be shown that only a flux of exactly $\Phi_0 \equiv h/2e \approx 2.07 \times 10^{-15}$ Wb, known as the flux quantum, may be allowed to enter the loop before superconductivity is restored, the voltage across the loop returns to zero and the process restarts. This causes the voltage to be periodic in the applied magnetic field, and by counting the number of periods one may determine the flux through the loop with extremely high resolution, owing to the small value of Φ_0. For this reason, SQUIDs are used to measure magnetic fields in applications where extreme sensitivity is required.

A third property of the SQUID is that, in the presence of an oscillating electric field, the voltage across the loop may increase in discrete steps (*Shapiro steps*) with increasing biasing current. This is a consequence of the AC Josephson effect, the phenomenon whereby the current in a Josephson junction naturally oscillates in time. While a rigorous explanation of this effect is well beyond the scope of the report, we will use the known result

$$\Phi_0 \equiv \frac{h}{2e} = \frac{\Delta V}{\nu} \tag{1}$$

to determine Φ_0 given the size ΔV of the voltage steps and the frequency ν of the oscillating electric field.

1b. Outline

In § 2, we will briefly describe the experimental setup and procedure. In § 3, we will present and analyse measurements of the SQUID's properties, beginning with its superconducting *I*-*V* characteristics in § 3a, followed by the periodic voltage-flux relationship in § 3b and the microwave-induced Shapiro steps in § 3c. In § 4 we will discuss the limitations of our work and suggest future improvements, before concluding the report in § 5.

2. Methods

The particular device tested in this work is the Star Cryoelectronics *Mr SQUID*, which uses a $Y_1Ba_2Cu_3O_7$ high-temperature superconducting film ($T_c \approx 90$ K). The reader is referred to the *Mr SQUID User's Guide* (Simon et al. 2012) for a detailed description.

The device was immersed in liquid nitrogen at 77 K. The biasing current and magnetic field were varied by a control

Corresponding author: Thomas Schanzer,
t.schanzer@student.unsw.edu.au
Word count: 2107

unit supplied by the device's manufacturer, with the current through and voltage across the device being measured and digitised by internal analog-to-digital converters before being sent to a computer for analysis. The oscillating electric field needed to create the Shapiro steps in § 3c was created by a signal generator connected to an antenna inside the dewar.

In § 3a and § 3c, the SQUID control unit was set to supply a triangle-wave biasing current and measure the resulting voltage, showing the relationship between the current and voltage in the device. In § 3b, the triangle-wave current was instead supplied to an internal coil in the SQUID, generating a proportional magnetic field and showing the relationship between voltage and flux.

3. Results

3a. I-V characteristics

Figure 2a shows the relationship between the biasing current and voltage across the SQUID. A clear superconducting region, where voltage is independent of current, is visible. Beyond some critical current, the superconductivity ceases and voltage varies approximately linearly with current.

The *normal resistance* of the device is the value of its resistance when the superconducting region is ignored, and is measured by finding the gradient between the endpoints of the I-V curve and doubling the result (because there are two Josephson junctions in parallel), as indicated by the grey line in Figure 2a. Since the curve is obviously nonlinear, the measured value can depend on the extent of the curve that is measured; one naturally asks what the horizontal distance between the endpoints should be. In Figure 2c, we show the slope between pairs of points (symmetric about the centre of the I-V curve) as a function of their horizontal separation ΔI and observe that the result converges to a fixed value, which we take to be the correct one. To reduce the effect of noise on the result, we use a cubic spline fit to the curve (the residuals of which are shown in Figure 2b) when computing slopes, and compare this to the slopes between the original data points in order to estimate the uncertainty. Our final result is

$$R_n = (1.75 \pm 0.01)\,\Omega, \tag{2}$$

which is larger than the value of 1.6 Ω measured by the manufacturer, possibly due to degradation of the device over several years of repeated cooling and warming.

In order to find the critical current at which superconductivity ceases, we model the transitions between the superconducting and normal regions of the I-V curve using hyperbolae of the form

$$(y - m_1 x - b_1)(y - m_2 x - b_2) = c. \tag{3}$$

One asymptote, $y = m_1 x + b_1$, slopes upwards to match the normal region, while the other, $y = m_2 x + b_2$, is horizontal, matching the superconducting region. The constant c determines the sharpness of the transition. Using orthogonal distance regression to fit (3) to the two bends, the critical current may then be determined from the point of intersection of the asymptotes. Figure 3 shows the results of this procedure; the hyperbola happens to be an excellent model, fitting the data with a coefficient of determination exceeding 0.99. Averaging the values from the left and right knees, we find that the critical current of the SQUID is

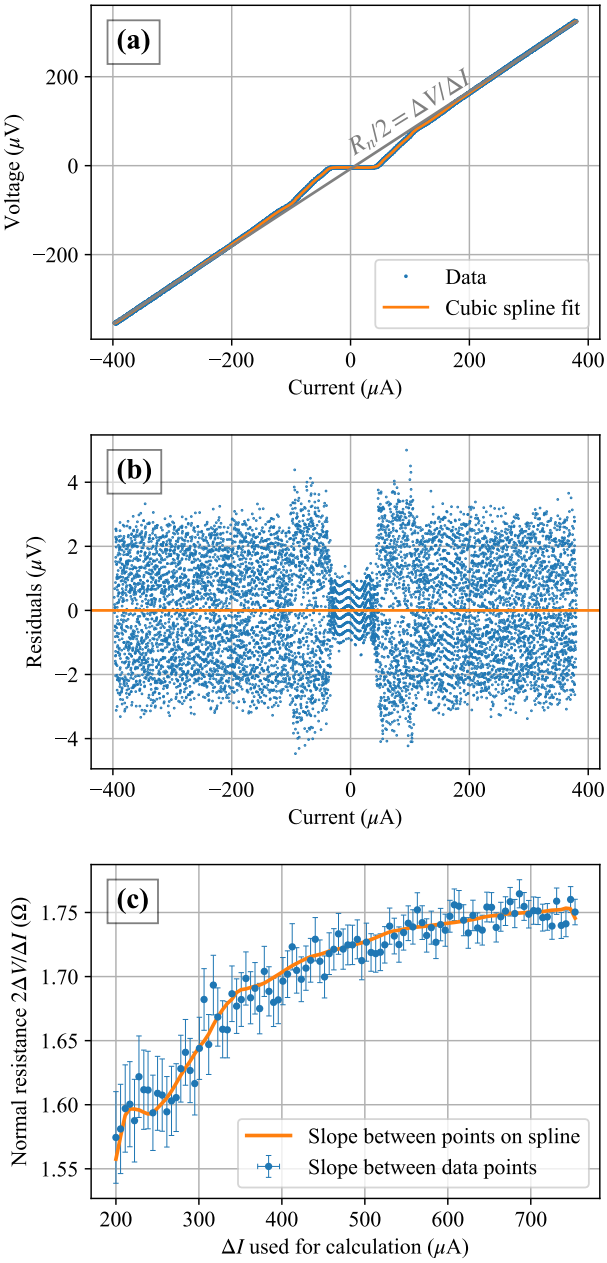

FIG. 2. **(a)**: I-V curve of the SQUID, with a cubic smoothing spline shown in orange. Current and voltage uncertainties for all data points were estimated to be 1 μA and 1 μV respectively. **(b)**: Residuals of the cubic spline fit. The non-uniformity of their magnitude is due to a contribution from the current uncertainty, which is larger in the upward-sloping regions. **(c)**: The normal resistance computed from the I-V curve as a function of the horizontal separation of the points used.

$$2I_c = (39.1 \pm 1.2)\,\mu\text{A}. \tag{4}$$

This deviates significantly from the value of 68 μA measured by the manufacturer approximately five years prior to our work; we also attribute this to degradation of the device over time.

It was also possible to apply a constant magnetic field to the SQUID during the I-V sweeps by passing a current through

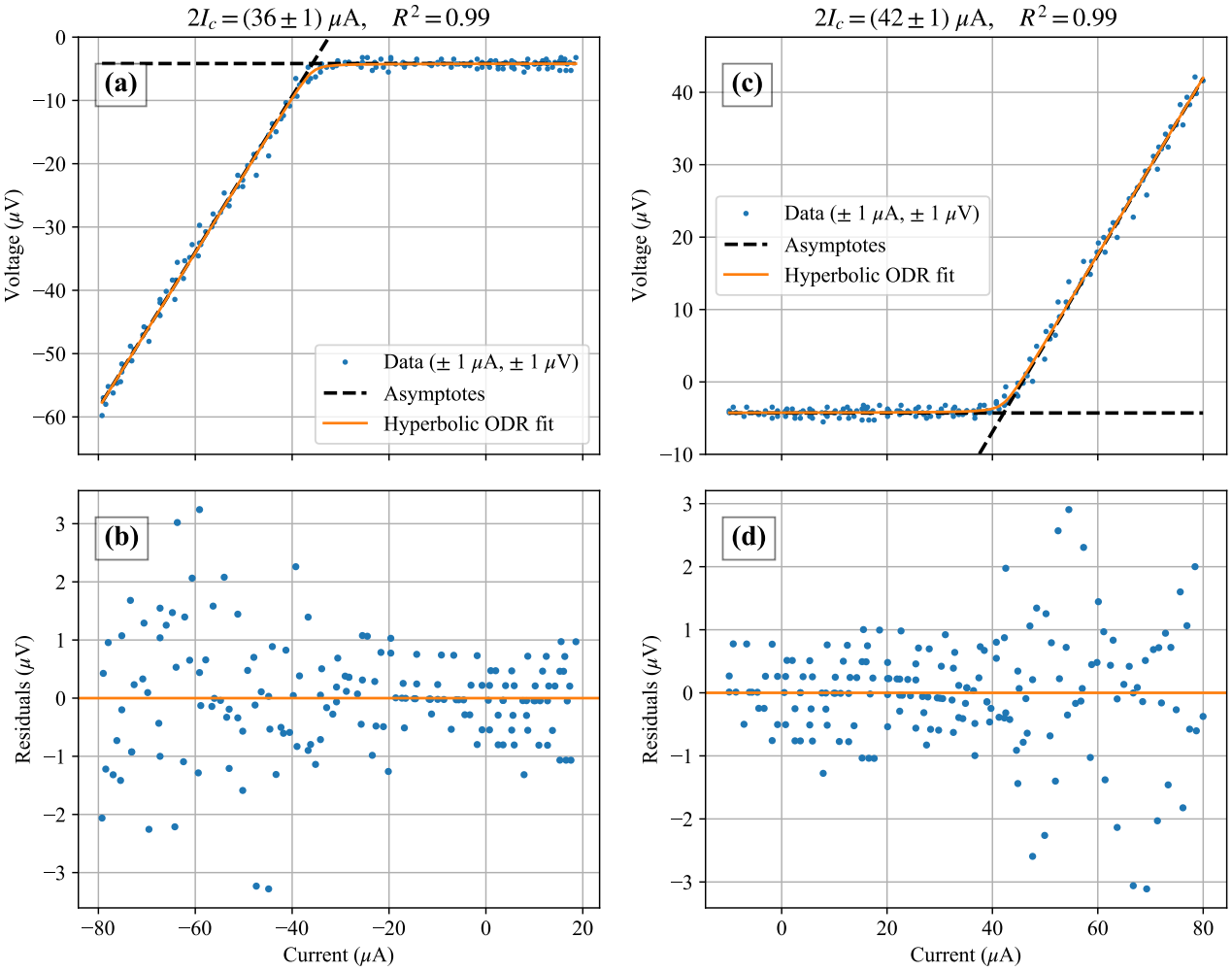

FIG. 3. **(a)**, **(c)**: hyperbolic fits to the bends in the I-V curve (orange), with asymptotes indicated by dashed black lines. The critical current $2I_c$ is the horizontal position of the intersection of the asymptotes. Error bars are omitted for clarity; the uncertainties in the x and y values are 1 µ and 1 µV respectively. **(b)**, **(d)**: residuals of the orange fits.

the internal feedback coil. The results shown in Figure 3 are for a coil current of 40 µA, which appeared to produce the sharpest transitions between the superconducting and normal regions. As an extension, I-V curves were acquired for a range of coil currents, allowing the measurement of critical current as a function of applied field. The result is shown in Figure 4; the critical current periodic in the applied field as anticipated in § 1. It also appears that setting the applied field so that the bends in the I-V curve are *less* sharp results in a higher critical current (at least according to the standard definition).

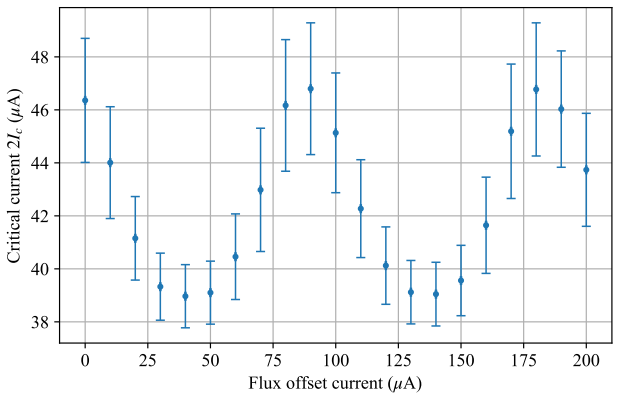

FIG. 4. Plot of critical current as a function of the current passed through the internal feedback coil, which is proportional to the applied magnetic field.

3b. V-Φ characteristics

Figure 5 shows the periodic variation of the voltage across the SQUID as the applied magnetic field (controlled by the current through an internal coil) is changed. By fitting a sinusoidal curve to the data using orthogonal distance regression, the peak-to-peak amplitude ΔV_Φ and period ΔI_Φ were determined.

The biasing current was set close to the critical current of the SQUID to ensure that changes in flux caused the induced current in the superconducting loop to momentarily exceed the critical current and allow a flux quantum to enter. It

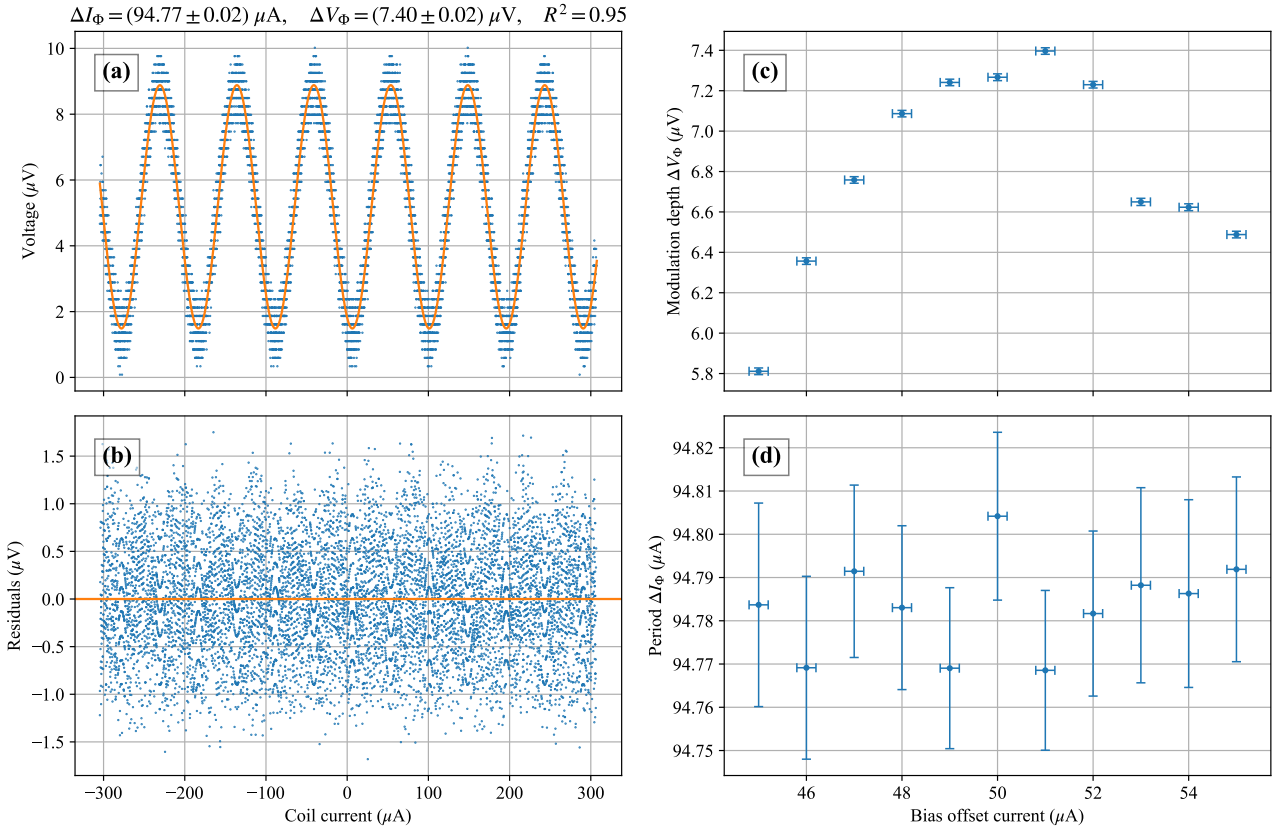

FIG. 5. **(a)**: Voltage across the SQUID as a function of the current through the internal feedback coil, which is proportional to the applied magnetic field. Error bars are omitted for clarity; current and voltage uncertainties for all data points were estimated to be 1 µA and 1 µV respectively. A sinusoidal ODR fit is shown in orange. **(b)**: Residuals of the sinusoidal fit in (a). **(c), (d)**: Plots of the peak-to-peak voltage amplitude and period, respectively, as functions of the bias current passing across the SQUID.

was observed that ΔV_Φ depended sensitively on the biasing current, while ΔI_Φ was constant, as shown in Figure 5c,d.

Unfortunately, the measured ΔV_Φ was at most (7.40 ± 0.02) µV, inconsistent with the manufacturer's value of 8.9 µV. ΔI_Φ, measured to be (94.78 ± 0.01) µA, was also inconsistent with the manufacturer's value of 97.5 µA. Both of these discrepancies could also be due to degradation of the device over time.

3c. Shapiro steps

Figure 6a shows the *I*-*V* curve of the SQUID in the presence of an external microwave-frequency electric field supplied by a signal generator. Three discrete steps in the voltage are observed as the biasing current is increased.

In order to determine Φ_0, we must determine the vertical separation ΔV between the steps, which in turn requires us to determine the positions of the steps. Recognising that the steps are the positions of minimum $\mathrm{d}V/\mathrm{d}I$, we fit a cubic spline to the *I*-*V* data and locate the minima in its derivative (the spline is used to reduce the noise in the data, which would be amplified by differentiation). Figure 6 shows three clear minima in the derivative as expected; we take the uncertainties in the positions to be the widths of the troughs at 10% of their depths. Mapped back onto the *I*-*V* curve, we obtain the step positions and uncertainties shown in Figures 6d,e,f, which appear very reasonable.

Finally, substitution of the positions into (1), given the microwave frequency 19.935 GHz, yields

$$\Phi_0 = \frac{h}{2e} = (2.05 \pm 0.04) \times 10^{-15}\ \mathrm{Wb}, \tag{5}$$

consistent with the accepted value of 2.068×10^{-15} Wb.

As an extension, the above procedure was repeated using *I*-*V* curves obtained at a range of microwave frequencies. Figure 7 shows a plot of the step size ΔV as a function of the frequency ν, producing a straight line whose slope should be equal to Φ_0. Since the uncertainty in frequency is negligible, ordinary least squares regression was used to fit a line to the points, yielding a slope

$$\Phi_0 = (2.07 \pm 0.08) \times 10^{-15}\ \mathrm{Wb}, \tag{6}$$

also consistent with the accepted value.

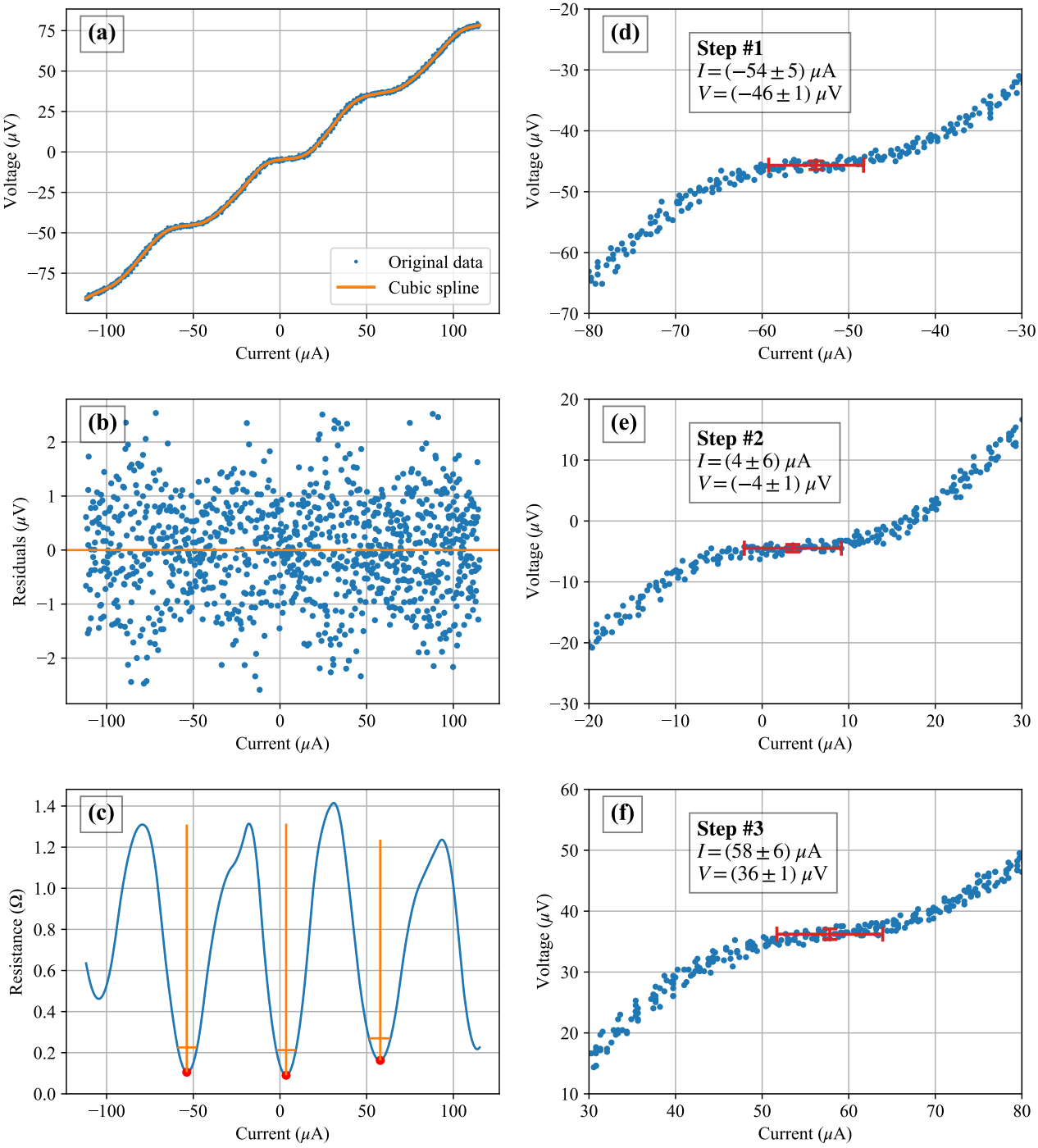

FIG. 6. **(a)**: the I-V curve of the SQUID when a 19.935 GHz oscillating electric field is applied, producing three Shapiro steps. Current and voltage uncertainties for all data points were estimated to be 1 μA and 1 μV respectively. A cubic spline fit is shown in orange. **(b)**: residuals of the cubic spline fit. **(c)**: the derivative of the cubic spline (blue curve), with three minima corresponding to the flat parts of the Shapiro steps. Vertical orange lines indicate the centres of the troughs, and the horizontal orange lines their widths at 10% of the trough depth. **(d)**, **(e)**, **(f)**: enlarged views of the three Shapiro steps, with the calculated positions of their centres indicated by red error bars.

4. Discussion

We shall now discuss some of the factors that affected the quality of our results. The most significant was the need to manually fine-tune the settings on the SQUID control unit (magnetic field and biasing current offset) in order to maximise the critical current in § 3a, the amplitude of the voltage oscillations in § 3b and the sharpness of the Shapiro steps in § 3c. The production of the Shapiro steps in § 3c also required time-consuming fine-tuning of the microwave frequency and power. While we have explored the dependence of our results on some of these settings (see Figures 4, 5c-d, 7); it appears that very small changes in the settings can significantly affect the measured SQUID parameters. In particular, it was found that a slight change in the position of

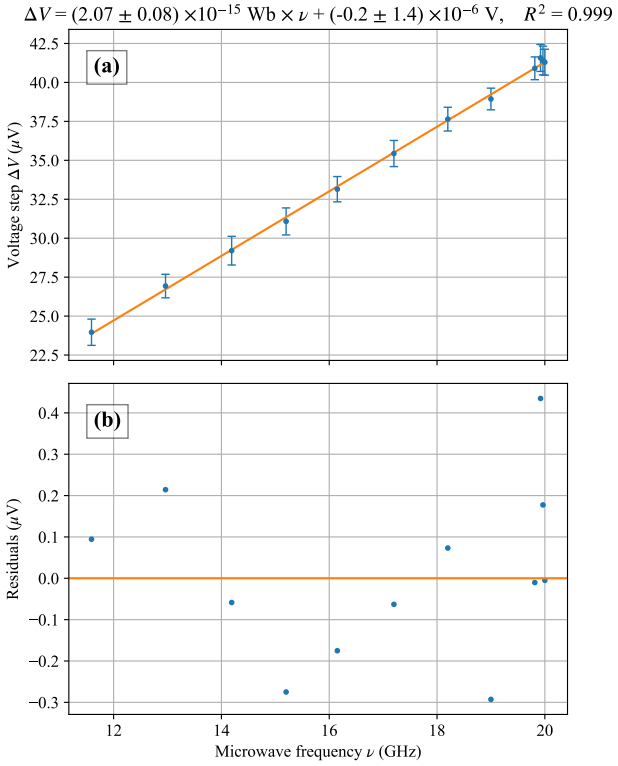

FIG. 7. **(a)**: Plot of the Shapiro voltage step size as a function of microwave frequency, with a least-squares linear fit in orange. The equation of the line is displayed above the plot. The uncertainty in frequency is negligible. **(b)**: Residuals of the fit in (a).

the microwave antenna inside the dewar could change the observed pattern of Shapiro steps. Consequently, it may be difficult to reproduce these results reliably in future work. A possible solution would be to use a remote-controllable measurement system that allows programmatic variation of the settings.

5. Conclusions

In § 3a we have measured the *I*-*V* characteristics of a SQUID, demonstrating and measuring the critical current threshold for superconductivity and measuring the normal resistance. The critical current was found to be a periodic function of applied magnetic field. The device also appears to have degraded over time, increasing the normal resistance and decreasing the critical current.

In § 3b, we showed that the voltage across the SQUID is a periodic function of applied magnetic field due to the quantisation of flux through the superconducting loop. There exists a particular biasing current that maximises the amplitude of the oscillations, but the bias current has no effect on the period.

Finally, in § 3c, we demonstrated that, in the presence of an oscillating electric field, the voltage across the device increases in discrete Shapiro steps when the biasing current is increased. By measuring the separation of the steps for a range of frequencies, we found the value of the magnetic flux quantum to be $\Phi_0 = h/2e = (2.07 \pm 0.08) \times 10^{-15}$ Wb, consistent with the accepted value and with reasonable precision.

In summary, we have successfully demonstrated and measured the properties of a SQUID. Our rigorous analysis techniques could be used to characterise other SQUIDs and are a step towards making precise magnetic field measurements using these sensitive devices.

Acknowledgments. The author thanks his laboratory partners J. Liang, A. Wei, T. Dunmore and D. Dunmore for their enlightening discussion of the experiment. In particular, he thanks J. Liang for suggesting the use of cubic spline fitting for finding the positions of the Shapiro steps in § 3c.

The author gratefully acknowledges the assistance of the UNSW School of Physics, which provided the facilities and equipment for this work, and the staff in the UNSW Higher Year Physics Laboratory, who provided guidance during the experiment.

Data availability statement. The raw data and Python code used to produce the results in this report are available as supplementary material at `https://github.com/tschanzer/SQUID`. They are also available from the author upon request.

References

Simon, R. W., M. J. Burns, M. S. Colclough, G. Zaharchuk, and R. Cantor, 2012: *Mr SQUID User's Guide*. 6.6 ed., Star Cryoelectronics.

APPENDIX

Voltage and current uncertainties

We briefly justify our claim that the uncertainties in our voltage and current measurements are approximately 1 µV and 1 µA respectively.

Figure A1 shows a plot of the triangle-wave current supplied through either the superconducting loop or the internal feedback coil. We fit a linear spline to it and find that the residuals of the fit are of order 1 µA, as claimed.

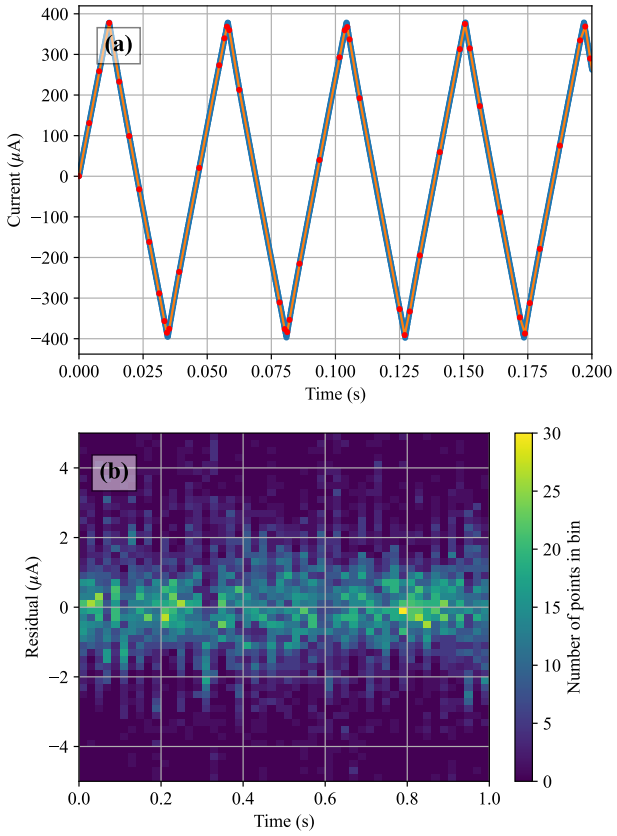

FIG. A1. **(a)**: Plot of the measured triangle-wave current (blue), with linear spline fit in orange. Red points indicate the knots of the spline. **(b)**: 2D histogram of the residuals, with the colour of each bin indicating the number of residual data points it contains. The key finding is that most of the residuals are within ±1 µA.

To determine the voltage uncertainty, we enlarge the superconducting potion of the *I*-*V* curve, where the voltage should be independent of current, in Figure A2. The data points in this region deviate vertically from the mean value by up to 1 µV, justifying our claim.

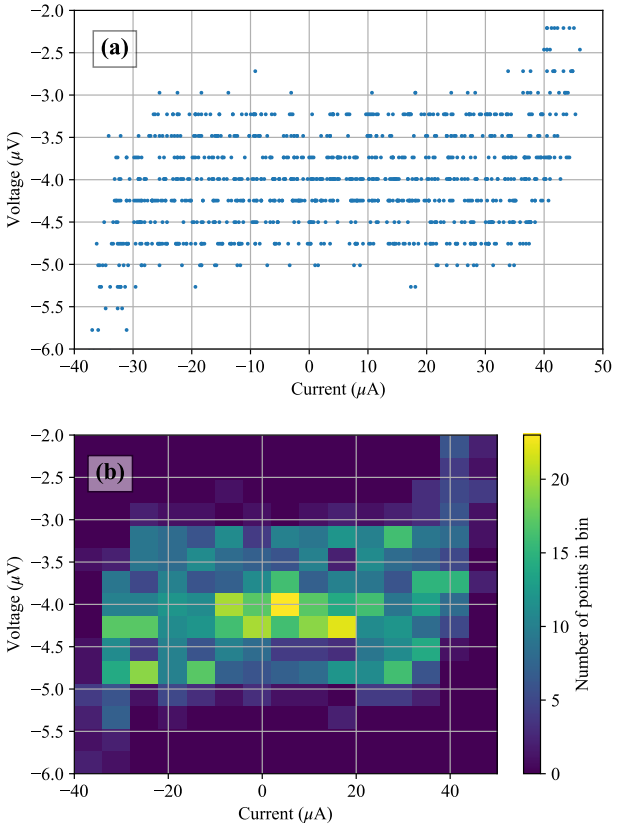

FIG. A2. **(a)**: Enlarged view of the superconducting region of the *I*-*V* curve. The appearance of several horizontal lines is due to the limited resolution of the analog-to-digital converter. Most points lie within 1 µV of the mean value at −4 µV. **(b)**: 2D histogram of the data points in (a), confirming the 1 µV uncertainty estimation.